N-Glycomic Profiling of Microsatellite Unstable Colorectal Cancer

Iiris Ukkola , Pirjo Nummela , Annamari Heiskanen , Matilda Holm , Sadia Zafar , Mia Kero , Caj Haglund , Tero Satomaa , Soili Kytölä , Ari Ristimäki *

Posted Date: 14 June 2023

doi: 10.20944/preprints202306.0975.v1

Keywords: BRAFV600E; colorectal cancer; microsatellite instability; mass spectrometry; N-glycosylation

Article

N-glycomic Profiling of Microsatellite Unstable Colorectal Cancer

Iiris Ukkola [1,2], Pirjo Nummela [1,2], Annamari Heiskanen [3], Matilda Holm [1,2,4,5]*, Sadia Zafar [1,2], Mia Kero [1], Caj Haglund [4,5] Tero Satomaa [3], Soili Kytölä [6] and Ari Ristimäki [1,2]**

1 Department of Pathology, HUSLAB, HUS Diagnostic Center, Helsinki University Hospital and University of Helsinki, Helsinki, Finland
2 Applied Tumor Genomics Research Program, Research Programs Unit, University of Helsinki and Helsinki University Hospital, Helsinki, Finland
3 Glykos Finland Ltd., Helsinki, Finland
4 Translational Cancer Medicine Research Program, Faculty of Medicine, University of Helsinki, Helsinki, Finland
5 Department of Surgery, Helsinki University Hospital and University of Helsinki, Helsinki, Finland
6 Department of Genetics, HUSLAB, HUS Diagnostic Center, Helsinki University Hospital and University of Helsinki, Helsinki, Finland
* **Current address:** Science for Life Laboratory, Department of Protein Science, KTH Royal Institute of Technology, Solna, Sweden and Department of Biosciences and Nutrition, Karolinska Institutet, Huddinge, Sweden.
* Correspondence: ari. ristimaki (at) helsinki. fi .

SIMPLE SUMMARY: All human cells have a complex glycan coating, and alterations in cell surface glycans play a role in cancer progression and immune suppression. Colorectal cancer is a heterogenous disease that can be classified into several molecular subtypes with major variances in prognosis and therapy responses. Two important molecular markers in this respect are microsatellite instability and BRAF gene mutation, which have been largely ignored in previous glycomics studies. We analyzed the N-glycan profiles of local and advanced colorectal cancers consisting of different molecular subtypes to identify possible explanations for their differing behavior. Our results show that the studied molecular subgroups of colorectal cancer have characteristic glycan profiles, which may explain their tumorigenic properties.

ABSTRACT: Aberrant glycosylation affects cancer progression and immune evasion. Approximately 15% of colorectal cancers (CRCs) demonstrate microsatellite instability (MSI) and display major differences in outcomes and therapeutic responses as compared to corresponding microsatellite stable (MSS) tumors. We compared the N-glycan profiles of stage II and IV MSI CRC tumors, further subdivided into $BRAF^{V600E}$ wild-type and mutated subgroups (n=10 in each subgroup), with each other and with those of paired non-neoplastic mucosal samples using mass spectrometry. Further, the N-glycans of $BRAF^{V600E}$ wild-type stage II MSI tumors were compared to corresponding MSS tumors (n=9). Multiple differences in N-glycan profiles were identified between MSI CRCs and control tissues, as well as between stage II MSI and MSS samples. MSI CRC tumors showed a lower relative abundance of high-mannose N-glycans than the control tissues or the MSS CRCs. Among MSI CRC subgroups, acidic N-glycans showed tumor stage and BRAF mutation status dependent variation. Especially large, sulfated/phosphorylated, and putative terminal N-acetylhexosamine containing acidic N-glycans differed between the MSI CRC subgroups, showing opposite changes in stage II and IV, when comparing BRAF mutated and wild-type tumors. Our results show that molecular subgroups of CRC have characteristic glycan profiles that may explain certain carcinogenic properties of MSI tumors.

Keywords: $BRAF^{V600E}$; colorectal cancer; microsatellite instability; mass spectrometry; N-glycosylation

1. Introduction

Colorectal cancer (CRC) is a heterogenous disease, which can be stratified by genomic and gene expression profiles into several distinct molecular subtypes with major differences in prognosis and

 doi:10.20944/preprints202306.0975.v1

therapeutic response. Approximately 15% of CRCs arise from microsatellite instability (MSI) pathway caused by deficient mismatch repair (dMMR) system, leading to hypermutation and increased cancer susceptibility. The MMR system can be compromised by epigenetic changes, usually by acquired *MLH1* promoter hypermethylation, or by genetic inactivation of *MLH1*, *MSH2*, *MSH6*, or *PMS2* genes characteristic to Lynch syndrome (LS) [1,2]. Among all CRC tumors, stage II-III MSI CRCs have a better prognosis than corresponding microsatellite stable (MSS) tumors, whereas stage IV MSI CRCs have a worse prognosis than corresponding MSS CRCs [1,2]. Further, *BRAF*^{V600E} mutation has been associated to aggressive behavior in MSS tumors but not in MSI tumors suggesting that the MSI phenotype may override the negative prognostic potential of *BRAF*^{V600E} mutation [3-6]. Immuno-oncological treatments with immune checkpoint inhibitors have shown excellent responses in advanced dMMR/MSI CRC patients [7,8] but only limited responses when treating MSS CRC patients [9,10]. Despite the clinical success, nearly half of metastatic dMMR/MSI CRCs fail to respond to immunotherapy [11,12]. The molecular mechanisms behind these differing responses are unclear.

All human cells have a complex glycan coating (the glycocalyx), which is involved in many essential cellular functions such as cell signaling, adhesion, differentiation, and proliferation [13,14]. Altered glycosylation, most often increased sialylation, fucosylation, and branching of N-linked glycans, has been observed in many types of cancer cells [13,14]. Aberrantly expressed glycans can modulate essential events of cancer development and progression, including angiogenesis, invasion and metastasis [13-15]. Further, the surface glycans of cancer cells play a role in evasion of immune response [16]. Glycan alterations may thus provide valuable novel molecular targets for cancer diagnostics and treatment.

N-glycan profiles of CRC tissues have previously been mainly compared with those of non-neoplastic colon tissues, and different stages of CRC have been compared without considering the MSI status. Increased glycosylation features in CRC include pauci-mannosidic, β1,6-branched, sulfated and sialylated N-glycans, especially α2,6-sialylated glycans, as well as glycans containing sialylated Lewis type epitopes [17, 18]. The decreased features in turn include structures with a bisecting N-acetylglucosamine [17,18]. In our previous study, we also demonstrated differences in the levels of sialylated and sulfated glycans between stage II and III right-sided CRC samples, with stage III tumors showing predominantly sulfated and stage II sialylated N-glycans [19]. Also, a study by Kaprio *et al*. showed pauci-mannose and small high-mannose N-glycan structures, as well as sialylated structures to be relatively more abundant in rectal carcinomas than adenomas [20].

The aim of this study was to analyze the N-glycan profiles of MSI CRC tumors to identify possible reasons for their differing behavior. We studied the neutral and acidic N-linked glycan profiles of MSI CRC samples (n=40) and pools of paired non-neoplastic colon controls (n=4) using MALDI-TOF mass spectrometry. The MSI CRC samples were further divided into subgroups according to the stage (II or IV) and BRAF^{V600E} mutation status (wt or mut) (n=10 in each group). In addition, the N-glycan profiles of stage II BRAFwt MSI tumors were compared to stage II BRAF^{V600E} wt MSS tumors (n= 9).

2. Materials and Methods

2.1. Tissue samples

Representative tissue samples from 40 MSI CRC patients were selected for the analysis. Of these patients, 38 had undergone surgical resection at Helsinki University Hospital (HUH) between 2018 and 2019, and the samples had been routinely screened for the MMR proteins MLH1, MSH2, MSH6, and PMS2 using immunohistochemistry (IHC). The selected samples showed loss of MLH1 expression (and concomitant loss of PMS2) and had also been routinely screened by BRAF^{V600E} IHC in real-life diagnostic setting. In addition, two MSI stage IV CRC samples from patients operated at HUH between 2014 and 2015 were included in the study. These samples were also dMLH1 by IHC and the BRAF^{V600E} status had been analyzed by next generation sequencing (NGS). The primary selection of MSI (dMLH1) CRC samples was done based on tumor stage (II or IV) and BRAF^{V600E} mutation status (mut or wt). Secondary selection was made based on patient age and sex, and tumor

 doi:10.20944/preprints202306.0975.v1

location (right or left side) to achieve similar study groups. For each of the MSI CRC subgroups (BRAFwt stage II, BRAFwt stage IV, BRAFmut stage II and BRAFmut stage IV), 10 samples were selected. In addition to the $BRAF^{V600E}$ IHC, the BRAF mutation status was confirmed by NGS in stage IV CRC samples and by droplet-digital polymerase chain reaction (ddPCR) in stage II samples. Further, a pool of paired non-neoplastic colon samples from each MSI CRC patient set (four pools, n=10 in each pool) was included in the glycomic profiling to serve as control tissues. For MSS reference sample set, we used our previously analyzed stage II MSS CRC samples [19]. From this published cohort, we selected only the stage II pMMR/MSS and BRAFwt cases (n=9) by using MMR and $BRAF^{V600E}$ IHC. These MSS stage II CRC patients had been operated at HUH between 2001 and 2003.

2.2. BRAF mutation analysis

$BRAF^{V600E}$ mutation status was confirmed by NGS in stage IV MSI CRC samples and by ddPCR in stage II MSI CRC samples. NGS analysis was done using an in-house cancer panel containing the *BRAF* exons 11-15 (in addition to the coding regions of *PIK3CA, EGFR, KIT, KRAS, MET, NRAS* and *PDGFRA*) and it was performed as previously described [21].

For the ddPCR analysis, targeted wild-type and *$BRAF^{V600E}$* mutation probes were designed and prevalidated by Bio-Rad (www.biorad.com) and 2 µl (100 ng) of the extracted DNA from formalin-fixed paraffin-embedded (FFPE) tissue samples was used for each duplicate reaction. Droplet generation and reading were performed according to the manufacturer's protocol using QX200 Droplet Generator and QX200 Droplet Reader (Bio-Rad, Hercules, CA, USA), respectively. The droplet generator first partitioned the samples for PCR amplification (22 µl into 20,000 droplets), and the droplets from each sample were then analyzed individually on the droplet reader. The data was processed with the QuantaSoft Analysis Pro Software (v.1.0; Bio-Rad).

2.3. N-glycan isolation

Representative areas of the carcinoma tissue or areas containing the highest percentages of epithelial cells in the paired non-neoplastic colon tissues were marked on HE slides, and macrodissection was used to cut 10 µm thick flakes from the FFPE tissue blocks with a Leica SM2000R microtome (Leica Microsystems GmbH, Wetzlar, Germany). After the last flake, a new HE slide was stained to verify the representativeness of the flakes. The tissue flakes were deparaffinized with xylene and rehydrated with descending ethanol series according to standard procedures, and N-linked glycans were liberated by N-glycosidase F (PNGase F) digestion (Glyko; ProZyme Inc., Hayward, CA) overnight at 37°C. N-glycan purification was then done as previously described [20] using the 96-well format. Briefly, the extracted glycans were passed in water through C_{18} silica and then absorbed into graphitized carbon material. The carbon wells were washed with water, and neutral N-linked glycans were eluted using 25% acetonitrile and acidic N-linked glycans with 0.05% trifluoroacetic acid in 25% acetonitrile in water. The acidic N-glycans were further purified with hydrophilic interaction solid-phase extraction. Both glycan fractions were then additionally passed in water through strong cation-exchange resin and C_{18} silica resin.

2.4. Mass spectrometry

Matrix-assisted laser desorption/ionization time-of-flight (MALDI-TOF) mass spectrometry (MS) was performed using a Bruker Ultraflex III TOF/TOF instrument (Bruker Daltonics Inc, Bremen, Germany) as previously described [20]. Neutral N-linked glycans were detected in positive ion reflector mode as $(M+Na)^+$ ions and acidic N-linked glycans in negative ion reflector mode as $(M-H)^-$ ions. Representative unprocessed MALDI TOF mass spectra of neutral and acidic N-linked glycans are shown in Supplementary Figure S1. The relative molar abundances of both neutral and acidic N-glycan components were assigned based on their relative signal intensities in the mass spectra when analyzed separately as neutral and acidic glycan fractions, and the unprocessed data was transformed into the present glycan profiles as previously described [22,23]. The resultant glycan

 doi:10.20944/preprints202306.0975.v1

signals in the glycan profiles were normalized to 100% to allow relative quantitative comparison between the samples. Normalized values were further assigned to structural/biosynthetic glycan classes based on their proposed monosaccharide composition as previously described [22,23]. All the relative abundances of both proposed monosaccharide compositions (glycans) and glycan classes are listed in Supplementary Tables S1 and S2. The mass spectrometry proteomics data of the previously analyzed stage II BRAF^{V600E} wt MSS CRC samples have been deposited to the ProteomeXchange Consortium via the PRIDE [24,25] partner repository with the dataset identifier PXD018673 (samples AH25-31-21-1/2, AH25-31-8-1/2, AH25-31-12-1/2, AH25-31-20-1/2, AH25-31-4-1/2, AH25-31-13-1/2, AH25-31-9-1/2, AH25-31-5-1/2 and AH25-31-37-1/2).

2.5. Analysis of N-linked glycan profiles

Statistical analysis of the N-linked glycan data was done in seven different study group settings between non-neoplastic colon samples (four pools of paired control samples), subgroups of MSI CRC samples according to the tumor stage and BRAF mutation status, and stage II BRAF^{V600E} wt MSI CRCs compared to stage II BRAF^{V600E} wt MSS tumors (Table 1). Both the relative abundances of proposed monosaccharide compositions and glycan classes were analyzed separately within these study groups. For statistical analyses, the nonparametric Kruskal-Wallis test was first used to verify the equality of the mean ranks of the groups and the Mann-Whitney U test with Benjamini-Hochberg false discovery rate (FDR) correction method [26] was then used for pairwise comparisons of the groups. RStudio (version 2022.07.2-576; Posit Software, Boston, MA) was used for statistical analyses and p-value <0.05 was considered statistically significant. The results are shown as mean relative abundance ± standard error of mean (SEM) for the separately calculated neutral and acidic N-glycan compositions and structural glycan classes.

Table 1. Seven different study groups analyzed for neutral and acidic N-glycans.

Number	Study group	n
1	Non-neoplastic controls vs. all MSI CRC	4 pools vs 40
2	CRC Stage II BRAFwt MSI vs MSS	10 vs 9
3	MSI CRC Stage II BRAFwt vs BRAFmut	10 vs 10
4	MSI CRC Stage II vs Stage IV	20 vs 20
5	MSI CRC BRAFwt Stage II vs IV	10 vs 10
6	MSI CRC BRAFmut Stage II vs IV	10 vs 10
7	MSI CRC Stage IV BRAFwt vs BRAFmut	10 vs 10

2.6. Immunohistochemistry

For IHC analyses, 4-µm sections cut from the FFPE tissue blocks were used. The MMR and BRAF^{V600E} IHC were performed as previously described [27,28].

3. Results

3.1. Clinicopathological characteristics of the CRC cases

Our study consisted of 40 MSI CRC samples, which were subdivided into four different subgroups (n=10 in each group) according to tumor stage (II or IV) and BRAF^{V600E} mutation status (wt or mut) (Table 1). Of these patients, the median age was 73 (range 51-89), 70% were females, and the tumors mainly localized to the right colon (80-100%) which are typical characteristics of MSI CRC patients (Table 2). MSI stage II tumors were mainly pT3 (70-80%) and low-grade (60%). MSI stage IV BRAFwt CRCs were more often high-grade (60% vs 30%) and pT4 (60% vs 30%) and displayed more often peritoneal metastasis (M1c, 40% vs 10%) when compared to MSI stage IV BRAFmut CRCs (Table 2). Stage IV MSI CRCs presented mainly synchronous metastases (16/20, 80%) and four cases were diagnosed with metachronous metastases in less than 6 months (2-5 months) of the follow-up. In the MSS stage II BRAFwt subgroup (n=9), a slight predominance of male sex (56%) and left-sided

 doi:10.20944/preprints202306.0975.v1

localization (56%) was seen, and the median age of the patients was 59 (range 52-77). Similar to MSI stage II CRCs, the MSS tumors were mainly pT3 (89%) and low-grade (78%) (Table 2).

Table 2. Characteristic of the CRC subgroups used in the study.

Subgroup			Subgroup		
All MSI CRC (n=40)	**Age**	**73 (51-89)**	**MSS CRC Stage II BRAFwt (n=9)**	Age	59 (52-77)
	Sex	♀ 28 (70%)		Sex	♀ 4 (44%)
		♂ 12 (30%)			♂ 5 (56%)
	Tumor site	R 35 (88%)		Tumor site	R 4 (44%)
		L 5 (12%)			L 5 (56%)
	Grade	LG 23 (58%)		Grade	LG 7 (78%)
		HG 17 (42%)			HG 2 (22%)
	pT	T2 1 (2%)		pT	T2 0 (0%)
		T3 25 (63%)			T3 8 (89%)
		T4 14 (35%)			T4 1 (11%)
	pN	N0 26 (65%)		pN	N0 9 (100%)
		N1 3 (7%)			N1 0 (0%)
		N2 11 (28%)			N2 0 (0%)
	M	M0 20 (50%)		M	M0 9 (100%)
		M1 20 (50%)			M1 0 (0%)
MSI CRC Stage II BRAFwt (n=10)	Age	72 (51-78)	**MSI CRC Stage II BRAFmut (n=10)**	Age	71 (58-82)
	Sex	♀ 7 (70%)		Sex	♀ 7 (70%)
		♂ 3 (30%)			♂ 3 (30%)
	Tumor site	R 8 (80%)		Tumor site	R 8 (80%)
		L 2 (20%)			L 2 (20%)
	Grade	LG 6 (60%)		Grade	LG 6 (60%)
		HG 4 (40%)			HG 4 (40%)
	pT	T3 7 (70%)		pT	T3 8 (80%)
		T4 3 (30%)			T4 2 (20%)
	pN	N0 10 (100%)		pN	N0 10 (100%)
	M	M0 10 (100%)		M	M0 10 (100%)
MSI CRC Stage IV BRAFwt (n=10)	Age	74 (54-86)	**MSI CRC Stage IV BRAFmut (n=10)**	Age	75 (63-89)
	Sex	♀ 7 (70%)		Sex	♀ 7 (70%)
		♂ 3 (30%)			♂ 3 (30%)
	Tumor site	R 9 (90%)		Tumor site	R 10 (100%)
		L 1 (10%)			L 0 (0%)
	Grade	LG 4 (40%)		Grade	LG 7 (70%)
		HG 6 (60%)			HG 3 (30%)
	pT	T2 1 (10%)		pT	T2 0 (0%)
		T3 3 (30%)			T3 7 (79%)
		T4 6 (60%)			T4 3 (30%)
	pN	N0 1 (10%)		pN	N0 5 (50%)
		N1 3 (30%)			N1 0 (0%)
		N2 6 (60%)			N2 5 (50%)
	M	M1a 4 (40%)		M	M1a 5 (50%)
		M1b 2 (20%)			M1b 4 (40%)
		M1c 4 (40%)			M1c 1 (10%)

 doi:10.20944/preprints202306.0975.v1

CRC, colorectal cancer; HG, high-grade; L, left; LG, low-grade; M, metastases; mut, mutated; N, nodes; MSI, microsatellite instability; MSS, microsatellite stable; R, right; T, tumor; wt, wild-type.

3.2. N-linked glycan profiles

3.2.1. N-glycan profiles of MSI CRC samples and paired non-neoplastic control samples

The major glycan types and structural features reported in this study are shown in Figure 1. Most of the differences between paired non-neoplastic colon samples (four pools) and MSI CRC samples (n=40) were detected in the neutral N-glycan profiles. Relative abundances of pauci-mannose, biantennary-size complex-type, monoantennary hybrid-type, fucosylated pauci-mannose (especially H2N2F1), and fucosylated hybrid-type glycans were significantly higher in MSI tumor samples than the controls (Table 3). Respective comparisons of monosaccharide compositions are shown in Supplementary Table S3. In contrast, the relative abundances of five N-acetylhexosamines (HexNAc=N) containing glycans (i.e. complex-type), high-mannose type glycans (e.g. compositions H6N2, H9N2, and H10N2), and a putative terminal HexNAc (N>H>1), containing glycans were significantly lower in MSI tumor samples than in controls (Table 3 and Supplementary Table S3). In addition, complex-type glycan structures with fucose and putative terminal HexNAc e.g. H3N5F1 and H4N5F1, as well as the putative bisecting (N=H≥5) N-acetylglucosamine structures H5N5F1 and H5N5F2 showed decreased abundances in MSI CRC as compared to the controls (Supplementary Table S3). In acidic N-glycan profiles, only fucosylated complex-type glycans showed significant change, i.e. a decrease in MSI CRCs as compared to the controls (Table 3). Further, several multifucosylated and putatively sulfated N-glycan structures (e.g. H5N4F3P1, H4N5F3P1, H5N5F2P1, H5N5F3P1 and H6N6F3P1) were less abundant in MSI tumor samples (Supplementary Table S3).

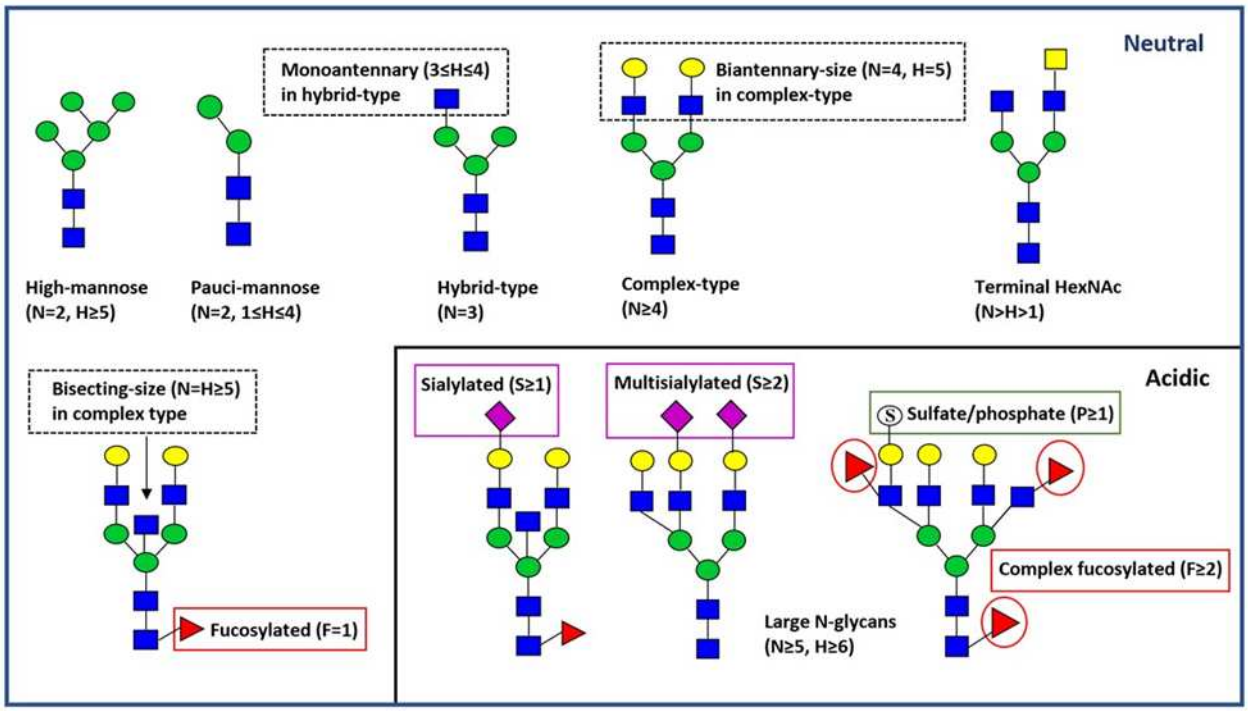

Figure 1. Major types and features of N-glycans. Representative N-glycan structures are depicted by green circle (D-mannose), blue square (N-acetyl-D-glucosamine), yellow square (N-acetyl-D-galactosamine, red triangle (L-fucose), yellow circle (D-galactose), purple diamond (N-acetylneuraminic acid, sialic acid), and open circles with an "S" (sulfate or phosphate ester). Major N-glycan structural classes are shown below the schematic structures. Further N-glycan structural

 doi:10.20944/preprints202306.0975.v1

features are indicated in boxes. H=hexose; N=N-acetylhexosamine=HexNAc; F=deoxyhexose (fucose), S=sialic acid; P=acid ester (sulfate/phosphate).

Table 3. Relative abundances of significantly different neutral and acidic N-glycan classes between controls (n=4 pools) and MSI CRC samples (n=40).

	Ctrls		MSI CRC		Fold change	p-adjusted[a]
	Average (%)	SEM	Average (%)	SEM		
NEUTRAL						
5 HexNAc	15.3	1.3	8.3	0.7	0.5	0.007
High-mannose type	40.2	2.6	33.0	1.2	0.8	0.039
Pauci-mannose type	15.5	1.3	24.1	1.2	1.6	0.045
Biantennary-size in complex-type	25.7	1.7	36.8	1.6	1.4	0.044
Monoantennary in hybrid-type	38.0	1.8	45.2	1.0	1.2	0.028
Fucosylation in pauci-mannose type	51.7	1.3	71.8	1.8	1.4	0.011
Fucosylation in hybrid-type	52.2	1.2	65.3	2.0	1.3	0.014
Terminal HexNAc	17.7	1.3	13.1	1.0	0.7	0.039
ACIDIC						
Fucosylation in complex-type	71.9	1.9	57.8	2.0	0.8	0.028

[a]Benjamini-Hochberg. CRC, colorectal cancer; HexNAc, N-acetylhexosamine; MSI, microsatellite instability; SEM, standard error of mean.

3.2.2. N-glycan profiles between stage II MSI and MSS samples

Neutral N-glycan profiles of MSI BRAFwt stage II CRC samples (n=10) were clearly different than those of our MSS BRAFwt stage II samples (n=9). MSI stage II CRC samples showed distinctively higher relative abundances of several neutral N-glycan classes, including complex-type glycans (4 HexNAc and 5 HexNAc), biantennary-size complex-type glycans, monoantennary hybrid-type glycans, and fucosylated glycans (especially fucosylated pauci-mannose type glycans e.g. H2N2F1), than the MSS samples (Table 4). Further, the putative terminal HexNAc containing glycan H3N4F1 and fucosylated complex-type glycans H4N4F1, H5N4F1, H5N5F1, and H6N5F1 were more abundant in MSI than in MSS samples (Supplementary Table S4). On the contrary, MSI Stage II CRC samples showed lower abundances of oligomannose structures (N2= 2 HexNAc, e.g. high-mannose type H5N2, H6N2, H7N2, and H8N2, and pauci-mannose type H2N2, H3N2, and H4N2), hybrid-type (3 HexNAc) and high-mannose type structures, as well as putative terminal HexNAc containing complex-type glycans, than MSS Stage II CRC (Table 4 and Supplementary Table S4).

Table 4. Relative abundances of significantly different neutral N-glycan classes between MSS BRAFwt stage II and MSI BRAFwt stage II samples.

	MSS St II BRAFwt		MSI St II BRAFwt		Fold change	p-adjusted[a]
	Average (%)	SEM	Average (%)	SEM		
2 HexNAc	74.1	3.0	54.8	5.0	0.7	0.005
3 HexNAc	6.4	0.4	4.8	0.3	0.8	0.016
4 HexNAc	9.5	1.2	29.1	4.7	3.1	0.001
5 HexNAc	4.6	1.0	8.5	1.4	1.8	0.030
High-mannose type	53.8	2.4	31.9	3.2	0.6	0.001
Complex type	16.8	2.5	40.4	4.9	2.4	0.002
Biantennary-size in complex-type	27.5	4.1	41.1	3.4	1.5	0.025
Monoantennary in hybrid-type	29.3	4.2	43.1	2.8	1.5	0.013
Fucosylation	25.6	2.3	50.5	5.1	2.0	0.006
Fucosylation in pauci-mannose type	43.0	3.0	69.9	5.5	1.6	0.005

 doi:10.20944/preprints202306.0975.v1

Terminal HexNAc in hybrid-type	1.5	1.0	3.1	0.3	2.1	0.040
Terminal HexNAc in complex-type	41.7	5.1	27.9	2.8	0.7	0.030

[a]Benjamini-Hochberg HexNAc, N-acetylhexosamine; MSI, microsatellite instability; MSS, microsatellite stabile; mut, mutated; SEM, standard error of mean; St, stage; wt, wild-type.

Acidic N-glycan profiles of the MSI BRAFwt stage II CRC samples versus corresponding MSS cases showed higher number of significantly different glycan classes than the neutral N-glycan profiles. Four HexNAc containing (N4) and biantennary-size complex-type N-glycans were relatively more abundant in MSI stage II CRC samples than in MSS stage II (Table 5), as well as the sialylated and multisialylated complex-type glycans S1H5N4F1, S1H5N4F2, S2H5N4, S2H5N4F1, S3H6N5 and S3H6N5F1 (Supplementary Table S5). Among the less abundant N-glycan classes in MSI stage II samples as compared to MSS stage II were hybrid-type glycans (3 HexNAc), and large N-glycans (≥5 HexNAc), as well as fucosylated and complex fucosylated glycans (both features especially in complex-type glycans, complex fucosylation also in hybrid-type), putative terminal HexNAc structures (especially in complex-type and bisecting size complex-type glycans), and acid ester-modified (sulfated/phosphorylated) hybrid-type N-glycans (Table 5).

Table 5. Relative abundances of significantly different acidic N-glycan classes between MSS BRAFwt stage II and MSI BRAFwt stage II samples.

	MSS St II BRAFwt		**MSI St II BRAFwt**		**Fold change**	**p-adjusted[a]**
	Average (%)	**SEM**	**Average (%)**	**SEM**		
3 HexNAc	10.0	1.3	1.9	0.5	0.2	0.002
4 HexNAc	41.9	4.3	74.6	3.6	1.8	0.002
5 HexNAc	19.8	1.0	13.8	0.8	0.7	0.001
6 HexNAc	14.9	1.9	5.4	1.5	0.4	0.007
7 HexNAc or larger	13.5	3.4	4.3	1.6	0.3	0.030
Complex-type	90.1	1.3	98.1	0.5	1.1	0.002
Biantennary-size in complex-type	42.9	4.7	75.5	3.5	1.8	0.002
Fucosylation	75.6	2.9	56.3	4.3	0.7	0.017
Fucosylation in complex-type	76.8	3.0	55.8	4.2	0.7	0.013
Complex fucosylation	35.0	5.2	12.6	2.6	0.4	0.011
Complex fucosylation in hybrid-type	16.1	5.2	1.5	1.5	0.1	0.011
Complex fucosylation in complex-type	36.9	5.3	12.8	2.7	0.3	0.011
Terminal HexNAc	20.9	5.4	2.0	0.8	0.1	0.004
Terminal HexNAc in complex-type	23.3	6.0	2.0	0.8	0.1	0.003
Terminal HexNAc (bisecting-size) in complex-type	14.0	2.8	5.3	2.0	0.4	0.017
Sulfate/phosphate in hybrid type	34.7	8.6	9.4	6.3	0.3	0.019

[a]Benjamini-Hochberg HexNAc, N-acetylhexosamine; MSI, microsatellite instability; MSS, microsatellite stabile; mut, mutated; SEM, standard error of mean; St, stage; wt, wild-type.

3.2.3. N-glycan profiles between BRAFwt and BRAFmut stage II MSI samples

When MSI stage II BRAFwt cases were compared to corresponding BRAFmut samples, only minor differences were seen in neutral N-glycan profiles, the fucosylated hybrid-type structures H2N3F1 and H3N3F1 being slightly increased in BRAFmut samples (Supplementary Table S6). The acidic N-glycan profiles in turn displayed more differences, with BRAFmut samples having increased relative abundances of 4 HexNAc and biantennary-size complex type glycans, as well as sialylated complex-type glycans (especially S2H5N4) (Table 6 and Supplementary Table S7). Among the less abundant glycan classes in BRAFmut stage II MSI samples were large N-glycans (≥5 HexNAc), and putative terminal HexNAc containing glycans, especially terminal HexNAc in complex-type and

 doi:10.20944/preprints202306.0975.v1

bisecting size complex-type glycans. (Table 6). Most interestingly, no sulfated/phosphorylated N-glycans were identified in any of the BRAFmut stage II MSI CRC samples, and all detected acidic N-glycans were thus sialylated (Table 6).

Table 6. Relative abundances of significantly different acidic N-glycan classes between MSI CRC subgroups.

	MSI St II BRAFwt		MSI St II BRAFmut			
	Average (%)	**SEM**	**Average (%)**	**SEM**	**Fold change**	**p-adjusted[a]**
4 HexNAc	74.6	3.6	93.2	1.2	1.2	0.002
5 HexNAc	13.8	0.8	4.7	0.6	0.3	0.001
6 HexNAc	5.4	1.5	0.6	0.2	0.1	0.007
7 HexNAc or larger	4.3	1.6	0.0	0.0	None in BRAFmut	0.001
Large N-glycans	21.9	2.9	4.7	0.7	0.2	0.001
Biantennary-size in complex-type	75.5	3.5	94.4	0.7	1.3	0.001
Terminal HexNAc	2.0	0.8	0.7	0.7	0.4	0.023
Terminal HexNAc in complex-type	2.0	0.8	0.7	0.7	0.4	0.023
Terminal HexNAc (bisecting-size) in complex-type	5.3	2.0	0.4	0.2	0.1	0.005
Sialylated	88.1	4.6	100.0	0.0	1.1	0.008
Sialylated complex-type	88.1	4.6	100.0	0.0	1.1	0.008
Sulfate or phosphate	12.0	4.6	0.0	0.0	None in BRAFmut	0.008
Sulfate/phosphate in complex-type	12.0	4.6	0.0	0.0	None in BRAFmut	0.008
	MSI St II		**MSI St IV**			
	Average (%)	**SEM**	**Average (%)**	**SEM**	**Fold change**	**p-adjusted[a]**
Biantennary-size in complex-type	84.9	2.8	78.0	2.9	0.9	0.038
	MSI St II BRAFwt		**MSI St IV BRAFwt**			
	Average (%)	**SEM**	**Average (%)**	**SEM**	**Fold change**	**p-adjusted[a]**
5 HexNAc	13.8	0.8	10.2	0.4	0.7	0.009
7 HexNAc or larger	4.3	1.6	0.4	0.2	0.1	0.030
Large N-glycans	21.9	2.9	12.3	0.7	0.6	0.020
Biantennary-size in complex-type	75.5	3.5	86.0	0.8	1.1	0.032
	MSI St II BRAFmut		**MSI St IV BRAFmut**			
	Average (%)	**SEM**	**Average (%)**	**SEM**	**Fold change**	**p-adjusted[a]**
4 HexNAc	93.2	1.2	69.7	4.3	0.7	0.001
5 HexNAc	4.7	0.6	16.5	1.6	3.5	0.001
6 HexNAc	0.6	0.2	7.7	1.9	12.8	0.002
7 HexNAc or larger	0.0	0.0	4.5	1.6	None in St II	0.001
Large N-glycans	4.7	0.7	23.1	3.1	4.9	0.001
Biantennary-size in complex-type	94.4	0.7	69.9	4.5	0.7	0.001
Terminal HexNAc	0.7	0.7	6.1	1.8	8.7	0.006
Terminal HexNAc in complex-type	0.7	0.7	6.2	1.8	8.9	0.006
Terminal HexNAc (bisecting-size) in complex-type	0.4	0.2	7.9	3.4	19.8	0.001
Sialylated	100.0	0.0	89.8	3.4	0.9	0.004
Sialylated complex-type	100.0	0.0	89.9	3.4	0.9	0.004
Sulfate/phosphate	0.0	0.0	10.7	3.4	None in St II	0.002
Sulfate/phosphate in complex-type	0.0	0.0	10.6	3.4	None in St II	0.002
	MSI St IV BRAFwt		**MSI St IV BRAFmut**			
	Average (%)	**SEM**	**Average (%)**	**SEM**	**Fold change**	**p-adjusted[a]**
4 HexNAc	85.2	0.8	69.7	4.3	0.8	0.002
5 HexNAc	10.2	0.4	16.5	1.6	1.6	0.005
6 HexNAc	2.0	0.6	7.7	1.9	3.9	0.005

 doi:10.20944/preprints202306.0975.v1

7 HexNAc or larger	0.4	0.2	4.5	1.6	11.3	0.011
Large N-glycans	12.3	0.7	23.1	3.1	1.9	0.001
Biantennary-size in complex-type	86.0	0.8	69.9	4.5	0.8	0.001
Terminal HexNAc	0.6	0.2	6.1	1.8	10.2	0.019
Terminal HexNAc in complex-type	0.6	0.2	6.2	1.8	10.3	0.019
Terminal HexNAc (bisecting-size) in complex-type	1.8	0.5	7.9	3.4	4.4	0.007
Sulfate/phosphate	1.8	1.7	10.7	3.4	5.9	0.019
Sulfate/phosphate in complex-type	1.8	1.7	10.6	3.4	5.9	0.019

[a]Benjamini-Hochberg HexNAc, N-acetylhexosamine; MSI, microsatellite instability; mut, mutated; SEM, standard error of mean; St, stage; wt, wild-type.

3.2.4. N-glycan profiles between stage II and stage IV MSI samples

Between all MSI Stage II samples and MSI stage IV samples (n=20 in both groups), only minor changes were seen in neutral or acidic N-glycan profiles. In neutral profiles, slight relative increases in hybrid-type glycans and fucosylated high-mannose type glycans, as well as the composition H3N4 (complex-type with putative terminal HexNAc), were detected in stage IV samples, whereas composition H7N6F1 (fucosylated complex-type) showed a slight decrease in stage IV samples (Table 7 and Supplementary Table S6). When acidic N-glycan classes were compared, only biantennary-size complex-type glycans showed a relative decrease in stage IV samples (Table 6). Of separate glycan structures, the sialylated S1H4N4F1 and the multisialylated S2H6N5 and S2H7N6F1 structures showed slightly higher relative abundance in MSI stage IV samples than in stage II samples (Supplementary Table S7).

Table 7. Relative abundances of significantly different neutral N-glycan classes between MSI subgroups.

	MSI St II		**MSI St IV**			
	Average (%)	**SEM**	**Average (%)**	**SEM**	**Fold change**	**p-adjusted[a]**
3 HexNAc	5.3	0.3	6.7	0.4	1.3	0.017
Fucosylation in high-mannose type	0.9	0.1	1.1	0.1	1.2	0.027
	MSI St II BRAFmut		**MSI St IV BRAFmut**			
	Average (%)	**SEM**	**Average (%)**	**SEM**	**Fold change**	**p-adjusted[a]**
Monoantennary in hybrid-type	49.5	1.1	41.6	1.3	0.8	0.008
	MSI St IV BRAFwt		**MSI St IV BRAFmut**			
	Average (%)	**SEM**	**Average (%)**	**SEM**	**Fold change**	**p-adjusted[a]**
Fucosylation in pauci-mannose type	77.3	1.2	66.0	3.9	0.9	0.024

[a]Benjamini-Hochberg HexNAc, N-acetylhexosamine; MSI, microsatellite instability; mut, mutated; SEM, standard error of mean; St, stage; wt, wild-type.

3.2.5. N-glycan profiles between stage II and stage IV in BRAFwt CRC

When MSI BRAFwt II samples were compared to corresponding stage IV samples, only minor relative changes were seen in neutral or acidic N-glycan profiles. In the neutral N-glycan profiles, only few separate monosaccharide compositions showed significant differences, e.g fucosylated hybrid-type structures H2N3F1 and H3N3F1 being more abundant in BRAFwt stage IV than stage II samples (Supplementary Table S6). In acidic N-glycan profiles, a higher abundance of biantennary-size complex type glycans, but clearly lower abundances of large-N-glycans (especially 5 HexNAc and 7 HexNAc or larger) were seen in the stage IV samples as compared to stage II (Table 6).

3.2.6. N-glycan profiles between stage II and stage IV in BRAFmut CRC

 doi:10.20944/preprints202306.0975.v1

Between MSI BRAFmut stage II and IV samples, neutral N-glycan profiles similarly showed only minor relative changes with monoantennary hybrid-type glycans and the fucosylated hybrid-type composition H2N3F1 being less abundant in BRAFmut stage IV samples than in stage II samples (Table 7 and Supplementary Table S6). More versatile relative differences were detected in the acidic N-glycan profiles of these MSI subgroups. In BRAFmut stage IV samples, large N-glycans, putative terminal HexNAc containing glycans (especially in complex-type and bisecting sized complex-type glycans) and sulfated/phosphorylated complex-type glycans were significantly more abundant than in stage II samples, whereas 4 HexNAc, biantennary-size complex-type, and sialylated complex-type glycans (especially S2H5N4) were relatively less abundant in BRAFmut stage IV than in stage II (Table 6 and Supplementary Table S7). Here it should be noted that the BRAFmut stage II MSI samples completely lacked the sulfated/phosphorylated N-glycans.

3.2.7. N-glycan profiles between BRAFwt and BRAFmut stage IV MSI samples

Finally, when comparing the neutral N-glycan profiles between MSI stage IV BRAFwt and BRAFmut samples, only fucosylated pauci-mannose glycans and the composition H2N3F1 (fucosylated hybrid-type glycan) showed significant difference, being less abundant in BRAFmut stage IV samples (Table 7 and Supplementary Table S6). The acidic profiles differed more, and in strict contrast to the differences between MSI Stage II BRAFwt and BRAFmut samples, the MSI stage IV BRAFwt and BRAFmut samples showed differences in the same glycan classes, but in the opposite direction (Figure 2). Stage IV BRAFmut samples thus showed higher relative abundances of large N-glycans and putative terminal HexNAc structures (especially in complex-type, and bisecting-size complex-type glycans), as well as sulfated/phosphorylated complex-type glycans but less 4 HexNAc and biantennary-size complex-type glycans than the BRAFwt stage IV samples (Table 6). The sialylated glycans were an exception, as those classes did not show significant differences between the stage IV subgroups. Of monosaccharide compositions, the sialylated complex-type structures S1H5N5F1 and S1H6N5 showed a slight increase in relative abundance, and S1H4N4F1 a decrease in stage IV BRAFmut when compared to corresponding BRAFwt samples (Supplementary Table S7).

 doi:10.20944/preprints202306.0975.v1

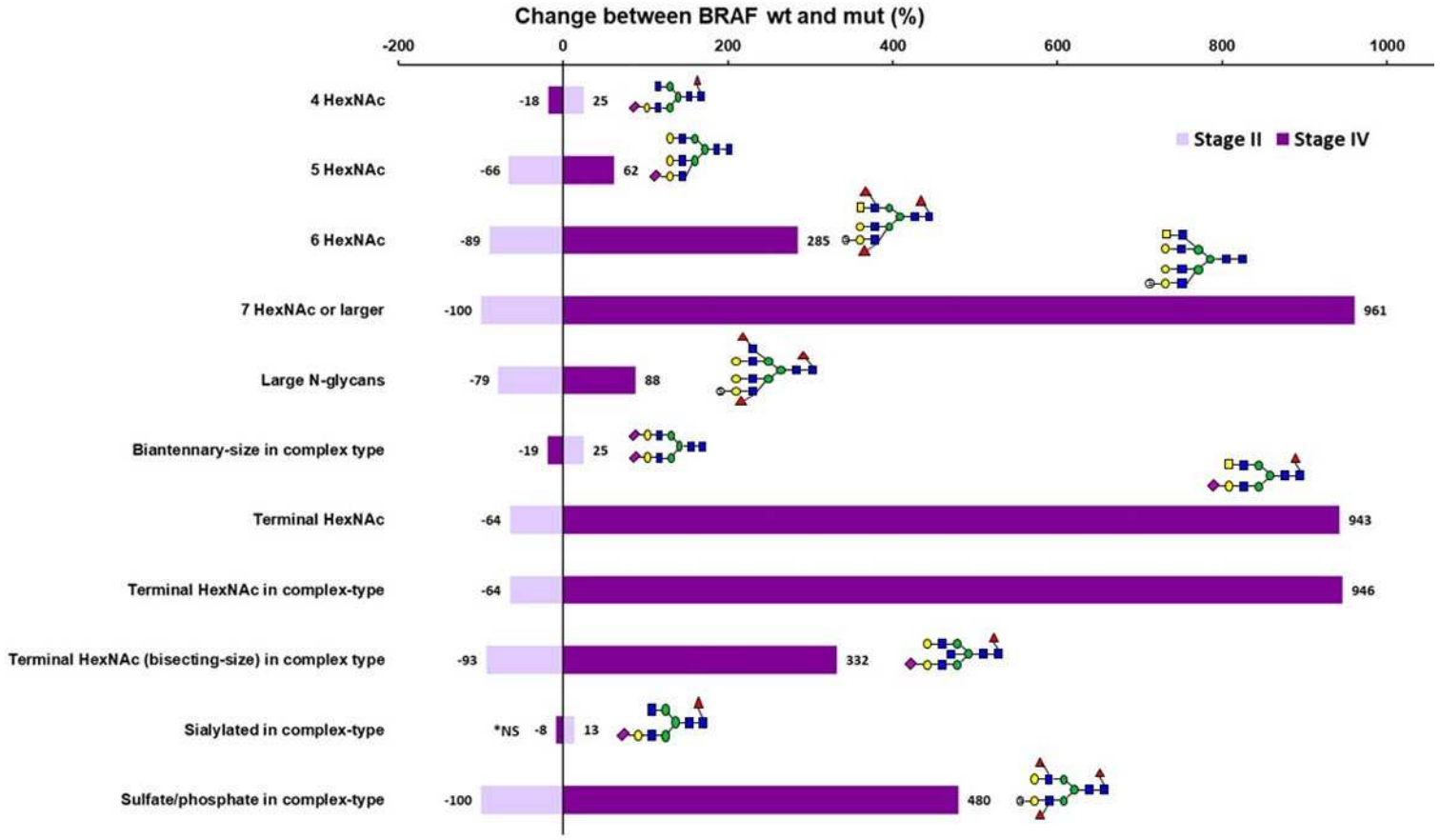

Figure 2. Change in the relative abundances of acidic N-glycan classes when comparing MSI BRAF^{V600E} wild-type and mutant CRC samples within the stage. The x-axis shows percentage increase or decrease in the relative abundances of the significantly different acidic N-glycan classes between BRAF wild-type and mutant samples within stage II (lavender) and stage IV (purple). Representative N-glycan structures are depicted by green circle (D-mannose), blue square (N-acetyl-D-glucosamine), yellow square (N-acetyl-D-galactosamine), red triangle (L-fucose), yellow circle (D-galactose), purple diamond (N-acetylneuraminic acid, sialic acid), and open circles with an "S" (sulfate or phosphate ester). *NS= not significant (in stage IV).

 doi:10.20944/preprints202306.0975.v1

4. Discussion

In this study, we investigated the N-linked glycan profiles of MSI CRC tissue specimens subdivided into subgroups according to stage (II or IV) and $BRAF^{V600E}$ mutation status (wt or mut) using MALDI-TOF mass spectrometry. Further, we compared these glycan profiles to those of both paired non-neoplastic colon tissue samples and MSS CRC specimens. We found multiple differences between MSI CRC samples and the control samples, and between MSI stage II and MSS stage II CRC samples. When MSI CRC subgroups were compared to each other, only minor differences were found in neutral N-glycan profiles, whereas a clear association between tumor stage and BRAF mutation status was seen in acidic N-glycan profiles. Most interestingly, no acid ester-modified (sulfated/phosphorylated) N-glycans were identified in any of the stage II MSI tumors with $BRAF^{V600E}$ mutation.

In line with previous glycomic profiling reports of CRC tissues [17-19], MSI CRC tumors showed a higher relative abundance of neutral pauci-mannose N-glycans, especially the fucosylated glycan H2N2F1, and decreased relative abundances of the putative terminal HexNAc (e.g. H3N5, H3N5F1, and H4N5F1) containing glycans, as well as the bisecting-size structure H5N5F1 as compared to the control tissues. In contrast to previous CRC reports, which have not specifically taken into account the MSI/MSS status [29-32], MSI tumors had a lower relative abundance of high-mannose type N-glycans than the non-neoplastic control tissues. Boyaval *et al.* [32] have demonstrated even higher levels of high-mannose type N-glycans in dysplastic regions of pre-cursor lesions than in early-stage CRC. Notably, in a recent study, overexpression of high-mannose N-glycans was demonstrated specifically in MSS CRC tumor tissue [33]. The acidic N-glycan profiles of MSI tumors were relatively simple, and, in contrast to previous reports, MSI tumors showed decreased relative abundances of some sulfated/phosphorylated and complex fucosylated structures e.g. H5N4F3P1 and H5N6F4P1 as compared to the control tissues [17,19]. Fucosylated neutral pauci-mannose and hybrid-type glycans were detected to increase but fucosylated acidic complex-type glycans to decrease in MSI CRC samples compared to non-neoplastic controls. Similarly, a higher abundance of fucosylated neutral N-glycans has been reported by Holm *et al*. [19] and a lower abundance of fucosylated complex-type N-glycans by Boyaval *et al*. [31] in CRC compared to adjacent normal colon epithelium. Further, we did not find any statistically significant difference in the abundances of sialylated N-glycans between MSI CRC samples and control tissues, whereas previous reports have reported increased levels of sialylation in CRC [17,29,31,34], and increased sialylation has also been attributed to metastatic potential and therapeutic resistance in CRC [35,36].

When comparing BRAFwt stage II MSI and MSS tumors, multiple significant differences were seen, both in neutral and acidic N-glycan profiles. MSI tumors showed distinctively higher relative abundances of neutral complex-type and monoantennary hybrid-type glycans, as well as fucosylation, especially in pauci-mannose glycans. On the contrary, clearly lower abundances of 2 HexNAc and high-mannose type glycans, as well as putative terminal HexNAc complex-type structures were observed in MSI than in MSS stage II tumors. In the acidic N-glycan profiles, MSI stage II BRAFwt tumors showed increased relative abundances of biantennary-size complex-type N-glycans and 4 HexNAc complex-type glycans than corresponding MSS samples. Yet, sulfated/phosphorylated hybrid-type glycans, large glycans and putative terminal HexNAc containing complex-type glycans, as well as fucosylated, especially fucosylated/complex fucosylated complex-type glycans were significantly less abundant in MSI stage II BRAFwt tumors. These neutral and acidic N-glycan types with differing abundances in MSI stage II CRC compared to corresponding MSS tumors, may be linked to the MSI pathway of CRC. To our knowledge this is the first study to report significant N-glycosylation differences between MSI and MSS CRC tissue samples.

Between MSI CRC subgroups, only minor differences were found in neutral N-glycan profiles and the major differences were observed in the acidic N-glycan profiles. Most interestingly, no sulfated/phosphorylated N-glycans were identified in any of the stage II MSI tumors containing $BRAF^{V600E}$ mutation. Between all MSI stage II and stage IV CRC, only acidic biantennary-size complex-type glycans showed a clear decrease in stage IV samples. When comparing MSI BRAFwt

 doi:10.20944/preprints202306.0975.v1

stage II and IV CRC samples to each other, biantennary-size complex type glycans were more abundant and large N-glycans less abundant in stage IV samples. Between BRAFmut stage II and stage IV samples, large N-glycans, putative terminal HexNAc containing and sulfated/phosphorylated complex-type glycans were significantly more abundant, and 4 HexNAc, biantennary-size complex-type and sialylated complex-type glycans less abundant in stage BRAFmut IV samples. Most interesting differences were observed when comparing MSI BRAFwt and BRAFmut samples within the stage. In these comparisons, the same glycan classes differed between BRAFwt and BRAFmut samples, but the direction of the change was totally opposite in stage II versus stage IV. In stage II BRAFmut samples, sulfated, large, and putative terminal HexNAc containing acidic N-glycans were decreased as compared to the corresponding BRAFwt samples, whereas in stage IV these same N-glycan features were increased in BRAFmut samples as compared to BRAFwt ones. On the other hand, increased levels of biantennary-size complex-type glycans, especially 4 HexNAc glycans were observed in stage II BRAFmut samples as compared to corresponding BRAFwt samples, whereas in stage IV samples these same glycan classes were decreased in BRAFmut samples relative to BRAFwt ones. $BRAF^{V600E}$ mutation is known to have a negative prognostic value in MSS CRC, while MSI has been suggested to override this negative effect [3,4,6]. Some studies have reported that BRAF mutation could be a positive prognostic marker in early stage MSI CRC [37] and, on the other hand, a negative prognostic factor in advanced MSI CRC [38,39]. The oppositely behaving acidic N-glycan types, especially large, sulfated/phosphorylated, and putative terminal HexNAc containing glycans, showed a clear dependency on tumor stage and BRAF mutation status and may thus be associated with MSI CRC progression according to BRAF mutation.

Large N-glycans commonly contain β1,6-branching, and increase in β1,6-branched N-linked glycans has been related to the malignant transformation and metastatic potential in many cancers, including CRC [13, 40- 42]. Importantly, the modification of epithelial cadherin (E-cadherin) with branched glycans is known to interfere cellular adhesion and promote tumour invasiveness and metastasis [13, 43]. Also, Kaprio *et al.* [20] has reported a significantly higher abundance of acidic N5 glycans in tissue samples of stage III CRC compared to stage I-II CRC samples. The enzyme catalyzing β1,6-branching of N-glycans is N-acetylglucosaminyltransferase V (GnT-V) encoded by the *MGAT5* gene. *MGAT5* expression is regulated by the RAS–RAF–MAPK pathway, and mutations of this oncogenic pathway are known to up-regulate GnT-V expression and concomitant β1,6-branching [13]. This is in line with our findings of increased levels of large (N≥5) acidic N-glycans in BRAFmut stage IV tumors as compared to corresponding BRAFwt ones but contradicts with BRAFmut stage II tumors showing lower levels of these glycans as compared to corresponding BRAFwt ones. Also, in our study, BRAFwt MSI stage II samples showed lower relative abundances of large acidic N-glycans than BRAFwt stage II MSS tumors thus potentially explaining for some degree the better prognosis of early stage MSI CRC as compared to corresponding MSS tumors.

Sulfated glycans have been shown to play an important role in many cell surface-related functions such as cellular adhesion and selectin-ligand interactions [44]. Higher levels of glycan-sulfotransferase activities have been demonstrated in poorly differentiated gastric carcinomas than in moderately differentiated ones, thus being associated with gastric tumorigenesis [45]. Also, sulfated Lewis X determinants form a predominant structural glycan motif in xenograft tumor mucin of LS174T-HM7 cells, a highly metastatic subline of the LS174T human CRC cell line [46]. Sulfated glycans are preferably bound by galectin-1 and galectin-2 [47], and upregulation of galectin-1 has been related to malignant progression in CRC [48,49]. In our study, sulfated/phosphorylated complex-type glycans were increased with the tumor stage in MSI BRAFmut samples, but not in MSI BRAFwt samples. Strikingly, sulfated/phosphorylated N-glycans were not found in any of the stage II MSI BRAFmut tumors whereas MSI BRAFwt stage II tumors displayed these glycans. Further, MSI stage II BRAFwt tumors showed a lower relative abundance of sulfated/phosphorylated hybrid-type glycans when compared to corresponding MSS samples.

Putative terminal HexNAc-containing N-glycans (N>H>1) have previously been identified in various CRC cell lines and increased abundances of terminal HexNAc residues have further been correlated with caudal-related homeobox protein 1 (CDX1) expressing CRC cells [50,51]. CDX1 is a

 doi:10.20944/preprints202306.0975.v1

transcription factor regulating normal development and differentiation of intestinal epithelium and associated with tumor suppressing potential in the colon [52]. More specifically, increased terminal N-acetylglucosamine (GlcNAc) has been identified in various carcinomas [22]. N-glycans containing bisecting GlcNAc have yet more been attributed to suppression of tumor progression and metastasis through regulation of cell surface glycoproteins such as stabilizing the E-cadherin mediated cell-cell adhesion [13,43]. N-glycans containing bisecting GlcNAc have also been reported to decrease in CRC tissue samples with more advanced tumor stages [30,34]. In our study, stage IV BRAFmut tumors showed in contrast higher relative abundances of acidic putative terminal HexNAc, especially in bisecting-size, containing complex-type glycans when compared to corresponding stage II samples. Although, a higher expression of bisecting N-glycans in a metastatic MSI CRC cell line (LIM1215) as compared with two non-metastatic MSI CRC cell lines (LIM1899 and LIM2405) has also controversially been demonstrated by Sethi *et al*. [53]. Further, the acidic putative terminal HexNAc and terminal HexNac in bisecting-size complex-type glycans showed significantly lower relative abundances in MSI stage II samples than in corresponding MSS samples.

A limitation of our study is that the mass spectrometric analyses were conducted using flakes from FFPE tissue blocks. It is thus not possible to specify from which cell type (e.g. cancer or stromal cells) the detached glycans originated. The tumor stroma is composed of various non-neoplastic cells e.g immune cells, fibroblasts and endothelial cells as well as extracellular matrix that forms a tumor microenvironment promoting cancer growth and spreading [54]. Moreover, the cancer related N-glycan signature has been demonstrated to spread into the stroma at the invasive front of the tumor [31]. We, however, used macrodissection to exclude the distant stroma and to achieve the highest percentage of epithelial cells in the carcinoma and non-neoplastic tissues. The analyzed tissues (tumor epithelium percentages 30-80%) although included varying amounts of tumor mucin, intra-tumor stroma and surrounding interface stroma which may contribute to the heterogeneity of the N-glycan signatures found in this study. Other limitation of this study is that we used pools of paired non-neoplastic colon samples from each MSI CRC patient set instead of individual paired non-neoplastic control samples. However, the main aim of this study was to compare the N-glycan profiles between MSI and MSS CRC samples and, especially, between different MSI CRC subgroups.

5. CONCLUSIONS

Our study identified multiple differences in N-glycan profiles between MSI tumors and control tissues, stage II MSI and MSS CRC samples, as well as within different MSI subgroups. Most importantly, we demonstrated that molecular subgroups of MSI CRCs have distinct glycan profiles that may explain certain carcinogenic characteristics of these CRC subtypes.

Supplementary Materials: Figure S1: Representative unprocessed MALDI-TOF mass spectra of (A) neutral and (B) acidic N-linked glycans isolated from a tumor tissue sample from a patient with stage II MSI $BRAF^{V600E}$ wild-type colon cancer. Note the different scales on y-axes. Table S1: MS data of acidic N-glycans, Table S2: MS data of neutral N-glycans, Table S3: Significantly different neutral and acidic monosaccharide compositions between controls (n=4 pools) and MSI CRC samples (n=40), Table S4: Significantly different neutral monosaccharide compositions between MSS BRAFwt stage II and MSI BRAFwt stage II samples, Table S5: Significantly different acidic monosaccharide compositions between MSS BRAFwt stage II and MSI BRAFwt stage II samples, Supplementary Table S6: Significantly different neutral monosaccharide compositions between MSI subgroups, Table S7: Significantly different acidic monosaccharide compositions between MSI subgroups.

Funding: This work was supported by Cancer Foundation Finland; Finska Läkaresällskapet; Helsinki University Central Hospital Research Funds; Medicinska Understödsföreningen Liv & Hälsa; Orion Research Foundation sr [IU]; Sigrid Jusélius Foundation; and the University of Helsinki. The funding sources had no role in study design, data collection and analysis, decision to publish, or preparation of the manuscript.

Acknowledgments: The authors thank Merja Haukka for excellent technical assistance.

Author Contributions: The study conception was contributed by Iiris Ukkola, Pirjo Nummela, and Ari Ristimäki. Data collection and material preparation were performed by Iiris Ukkola, Pirjo Nummela, Mia Kero, Matilda Holm, Soili Kytölä, Caj Haglund, and Ari Ristimäki. The data curation was contributed by Annamari Heiskanen and Tero Satomaa and formal analysis by Iiris Ukkola, Annamari Heiskanen, Tero Satomaa and Sadia Zafar. All authors had a role in detailed analysis of the data. Visualization of the manuscript was performed by Iiris Ukkola,

Pirjo Nummela and Tero Satomaa. The original draft of the manuscript was written by Iiris Ukkola, Pirjo Nummela and Ari Ristimäki and all authors commented on previous versions of the manuscript. All authors reviewed and approved the final manuscript.

Institutional Review Board Statement: The study was conducted according to the guidelines of the Declaration of Helsinki and approved by the Ethics Committee of the Helsinki University Central Hospital (DNRO 239/13/03/02/2011, 9.11.2011). A**ll methods were performed in accordance with the relevant guidelines and regulations**. Data were anonymized prior to use for the study.

Informed Consent Statement: Informed consent is not required by national regulations for research with de-identified samples and data.

Data Availability Statement: Data is contained within the article or Supplementary Materials.

Conflicts of Interest: All authors declare no conflict of interest.

References

1. Gupta, R.; Sinha, S.; Paul, R. N. The Impact of Microsatellite Stability Status in Colorectal Cancer. *Curr Probl Cancer* **2018**, *42*, 548-559; DOI:10.1016/j.currproblcancer.2018.06.010.
2. Diao, Z.; Han, Y.; Chen, Y.; Zhang, R.; Li, J. The Clinical Utility of Microsatellite Instability in Colorectal Cancer. *Crit Rev Oncol Hematol* **2021**, *157*, 103171; DOI:10.1016/j.critrevonc.2020.103171.
3. Seppälä, T. T.; Böhm, J. P.; Friman, M.; Lahtinen, L.; Väyrynen, V. M. J.; Liipo, T. K. E.; Ristimäki, A. P.; Kairaluoma, M. V. J.; Kellokumpu, I. H.; Kuopio, T. H. I.; Mecklin, J.-P. Combination of Microsatellite Instability and BRAF Mutation Status for Subtyping Colorectal Cancer. *Br J Cancer* **2015**, *112*, 1966–1975; DOI:10.1038/bjc.2015.160.
4. Bläker, H.; Alwers, E.; Arnold, A.; Herpel, E.; Tagscherer, K. E.; Roth, W.; Jansen, L.; Walter, V.; Kloor, M.; Chang-Claude, J.; Brenner, H.; Hoffmeister, M. The Association Between Mutations in BRAF and Colorectal Cancer–Specific Survival Depends on Microsatellite Status and Tumor Stage. *Clinical Gastroenterology and Hepatology* **2019**, *17*, 455-462.e6; DOI:10.1016/j.cgh.2018.04.015.
5. Fanelli, G. N.; Dal Pozzo, C. A.; Depetris, I.; Schirripa, M.; Brignola, S.; Biason, P.; Balistreri, M.; Dal Santo, L.; Lonardi, S.; Munari, G.; Loupakis, F.; Fassan, M. The Heterogeneous Clinical and Pathological Landscapes of Metastatic Braf-Mutated Colorectal Cancer. *Cancer Cell Int* **2020**, *20*, 30; DOI:10.1186/s12935-020-1117-2.
6. Offermans, K.; Jenniskens, J. C. A.; Simons, C. C. J. M.; Samarska, I.; Fazzi, G. E.; van der Meer, J. R. M.; Smits, K. M.; Schouten, L. J.; Weijenberg, M. P.; Grabsch, H. I.; van den Brandt, P. A. Association between Mutational Subgroups, Warburg-Subtypes, and Survival in Patients with Colorectal Cancer. *Cancer Med* **2023**, *12*, 1137-1156; DOI:10.1002/cam4.4968.
7. Luchini, C.; Bibeau, F.; Ligtenberg, M. J. L.; Singh, N.; Nottegar, A.; Bosse, T.; Miller, R.; Riaz, N.; Douillard, J.-Y.; Andre, F.; Scarpa, A. ESMO Recommendations on Microsatellite Instability Testing for Immunotherapy in Cancer, and Its Relationship with PD-1/PD-L1 Expression and Tumour Mutational Burden: A Systematic Review-Based Approach. *Annals of Oncology* **2019**, *30*, 1232–1243; DOI:10.1093/annonc/mdz116.
8. Yoshino, T.; Pentheroudakis, G.; Mishima, S.; Overman, M. J.; Yeh, K.-H.; Baba, E.; Naito, Y.; Calvo, F.; Saxena, A.; Chen, L.-T.; Takeda, M.; Cervantes, A.; Taniguchi, H.; Yoshida, K.; Kodera, Y.; Kitagawa, Y.; Tabernero, J.; Burris, H.; Douillard, J.-Y. JSCO—ESMO—ASCO—JSMO—TOS: International Expert Consensus Recommendations for Tumour-Agnostic Treatments in Patients with Solid Tumours with Microsatellite Instability or NTRK Fusions. *Annals of Oncology* **2020**, *31*, 861-872; DOI: 10.1016/j.annonc.2020.03.299.
9. Golshani, G.; Zhang, Y. Advances in Immunotherapy for Colorectal Cancer: A Review. *Therap Adv Gastroenterol* **2020**, *13*, 1756284820917527; DOI: 10.1177/1756284820917527.
10. Carlsen, L.; Huntington, K. E.; El-Deiry, W. S. Immunotherapy for Colorectal Cancer: Mechanisms and Predictive Biomarkers. *Cancers (Basel)* **2022**, *14*, 1028; DOI:10.3390/cancers14041028.
11. Ganesh, K.; Stadler, Z. K.; Cercek, A.; Mendelsohn, R. B.; Shia, J.; Segal, N. H.; Diaz, L. A. Immunotherapy in Colorectal Cancer: Rationale, Challenges and Potential. *Nat Rev Gastroenterol Hepatol* **2019**, *16*, 361–375; DOI:10.1038/s41575-019-0126-x.
12. Sveen, A.; Kopetz, S.; Lothe, R. A. Biomarker-Guided Therapy for Colorectal Cancer: Strength in Complexity. *Nat Rev Clin Oncol* **2020**, *17*, 11–32; DOI:10.1038/s41571-019-0241-1.
13. Pinho, S. S.; Reis, C. A. Glycosylation in Cancer: Mechanisms and Clinical Implications. *Nat Rev Cancer* **2015**, *15*, 540–555; DOI:10.1038/nrc3982.
14. Mereiter, S.; Balmaña, M.; Campos, D.; Gomes, J.; Reis, C. A. Glycosylation in the Era of Cancer-Targeted Therapy: Where Are We Heading? *Cancer Cell* **2019**, *36*, 6–16; DOI:10.1016/j.ccell.2019.06.006.
15. Marth, J. D.; Grewal, P. K. Mammalian Glycosylation in Immunity. *Nat Rev Immunol* **2008**, *8*, 874–887; DOI:10.1038/nri2417.

16. Läubli, H.; Borsig, L. Altered Cell Adhesion and Glycosylation Promote Cancer Immune Suppression and Metastasis. *Front Immunol* **2019**, *10*, 2120; DOI:10.3389/fimmu.2019.02120.
17. Balog, C. I. A.; Stavenhagen, K.; Fung, W. L. J.; Koeleman, C. A.; McDonnell, L. A.; Verhoeven, A.; Mesker, W. E.; Tollenaar, R. A. E. M.; Deelder, A. M.; Wuhrer, M. N-Glycosylation of Colorectal Cancer Tissues. *Mol Cell Proteomics* **2012**, *11*, 571–585; DOI:10.1074/mcp.M111.011601.
18. Sethi, M. K.; Fanayan, S. Mass Spectrometry-Based N-Glycomics of Colorectal Cancer. *Int J Mol Sci* **2015**, *16*, 29278–29304; DOI:10.3390/ijms161226165.
19. Holm, M.; Nummela, P.; Heiskanen, A.; Satomaa, T.; Kaprio, T.; Mustonen, H.; Ristimäki, A.; Haglund, C. N-Glycomic Profiling of Colorectal Cancer According to Tumor Stage and Location. *PLoS ONE* **2020**, *15*, e0234989; DOI:10.1371/journal.pone.0234989.
20. Kaprio, T.; Satomaa, T.; Heiskanen, A.; Hokke, C. H.; Deelder, A. M.; Mustonen, H.; Hagström, J.; Carpen, O.; Saarinen, J.; Haglund, C. N-Glycomic Profiling as a Tool to Separate Rectal Adenomas from Carcinomas. *Mol Cell Proteomics* **2015**, *14*, 277-288; DOI:10.1074/mcp.M114.041632.
21. Holm, M.; Andersson, E.; Osterlund, E.; Ovissi, A.; Soveri, L.-M.; Anttonen, A.-K.; Kytölä, S.; Aittomäki, K.; Osterlund, P.; Ristimäki, A. Detection of KRAS Mutations in Liquid Biopsies from Metastatic Colorectal Cancer Patients Using Droplet Digital PCR, Idylla, and next Generation Sequencing. *PLoS One* **2020**, *15*, e0239819; DOI:10.1371/journal.pone.0239819.
22. Satomaa, T.; Heiskanen, A.; Leonardsson, I.; Ångström, J.; Olonen, A.; Blomqvist, M.; Salovuori, N.; Haglund, C.; Teneberg, S.; Natunen, J.; Carpén, O.; Saarinen, J. Analysis of the Human Cancer Glycome Identifies a Novel Group of Tumor-Associated N-Acetylglucosamine Glycan Antigens. *Cancer Research* **2009**, *69*, 5811–5819; DOI:10.1158/0008-5472.CAN-08-0289.
23. Satomaa, T.; Heiskanen, A.; Mikkola, M.; Olsson, C.; Blomqvist, M.; Tiittanen, M.; Jaatinen, T.; Aitio, O.; Olonen, A.; Helin, J.; Hiltunen, J.; Natunen, J.; Tuuri, T.; Otonkoski, T.; Saarinen, J.; Laine, J. The N-Glycome of Human Embryonic Stem Cells. *BMC Cell Biology* **2009**, *10*, 42; DOI:10.1186/1471-2121-10-42
24. Deutsch, E. W.; Csordas, A.; Sun, Z.; Jarnuczak, A.; Perez-Riverol, Y.; Ternent, T.; Campbell, D. S.; Bernal-Llinares, M.; Okuda, S.; Kawano, S.; Moritz, R. L.; Carver, J. J.; Wang, M.; Ishihama, Y.; Bandeira, N.; Hermjakob, H.; Vizcaíno, J. A. The ProteomeXchange Consortium in 2017: Supporting the Cultural Change in Proteomics Public Data Deposition. *Nucleic Acids Res* **2017**, *45* (Database issue), D1100-D1106; DOI:10.1093/nar/gkw936.
25. Perez-Riverol, Y.; Bai, J.; Bandla, C.; García-Seisdedos, D.; Hewapathirana, S.; Kamatchinathan, S.; Kundu, D. J.; Prakash, A.; Frericks-Zipper, A.; Eisenacher, M.; Walzer, M.; Wang, S.; Brazma, A.; Vizcaíno, J. A. The PRIDE Database Resources in 2022: A Hub for Mass Spectrometry-Based Proteomics Evidences. *Nucleic Acids Res* **2021**, *50* (D1), D543–D552; DOI:10.1093/nar/gkab1038.
26. Benjamini, Y.; Hochberg, Y. Controlling the False Discovery Rate: A Practical and Powerful Approach to Multiple Testing. *Journal of the Royal Statistical Society. Series B (Methodological)* **1995**, *57*, 289–300; DOI:10.1111/j.2517-6161.1995.tb02031.x.
27. Thiel, A.; Heinonen, M.; Kantonen, J.; Gylling, A.; Lahtinen, L.; Korhonen, M.; Kytölä, S.; Mecklin, J.-P.; Orpana, A.; Peltomäki, P.; Ristimäki, A. BRAF Mutation in Sporadic Colorectal Cancer and Lynch Syndrome. *Virchows Arch* **2013**, *463*, 613–621; DOI:10.1007/s00428-013-1470-9.
28. Ukkola, I.; Nummela, P.; Pasanen, A.; Kero, M.; Lepistö, A.; Kytölä, S.; Bützow, R.; Ristimäki, A. Detection of Microsatellite Instability with Idylla MSI Assay in Colorectal and Endometrial Cancer. *Virchows Arch* **2021**, *479*, 471–479; DOI:10.1007/s00428-021-03082-w.
29. Sethi, M. K.; Hancock, W. S.; Fanayan, S. Identifying *N* -Glycan Biomarkers in Colorectal Cancer by Mass Spectrometry. *Acc. Chem. Res.* **2016**, *49*, 2099–2106; DOI:10.1021/acs.accounts.6b00193.
30. Zhang, D.; Xie, Q.; Wang, Q.; Wang, Y.; Miao, J.; Li, L.; Zhang, T.; Cao, X.; Li, Y. Mass Spectrometry Analysis Reveals Aberrant N-Glycans in Colorectal Cancer Tissues. *Glycobiology* **2019**, *29*, 372–384; DOI:10.1093/glycob/cwz005.
31. Boyaval, F.; van Zeijl, R.; Dalebout, H.; Holst, S.; van Pelt, G.; Fariña-Sarasqueta, A.; Mesker, W.; Tollenaar, R.; Morreau, H.; Wuhrer, M.; Heijs, B. N-Glycomic Signature of Stage II Colorectal Cancer and Its Association With the Tumor Microenvironment. *Mol Cell Proteomics* **2021**, *20*, 100057; DOI:10.1074/mcp.RA120.002215.
32. Boyaval, F.; Dalebout, H.; Van Zeijl, R.; Wang, W.; Fariña-Sarasqueta, A.; Lageveen-Kammeijer, G. S. M.; Boonstra, J. J.; McDonnell, L. A.; Wuhrer, M.; Morreau, H.; Heijs, B. High-Mannose N-Glycans as Malignant Progression Markers in Early-Stage Colorectal Cancer. *Cancers (Basel)* **2022**, *14*, 1552; DOI:10.3390/cancers14061552.
33. Coura, M. de M. A.; Barbosa, E. A.; Brand, G. D.; Bloch, C.; de Sousa, J. B. Identification of Differential N-Glycan Compositions in the Serum and Tissue of Colon Cancer Patients by Mass Spectrometry. *Biology (Basel)* **2021**, *10*, 343; DOI:10.3390/biology10040343.
34. Sethi, M. K.; Kim, H.; Park, C. K.; Baker, M. S.; Paik, Y.-K.; Packer, N. H.; Hancock, W. S.; Fanayan, S.; Thaysen-Andersen, M. In-Depth *N* -Glycome Profiling of Paired Colorectal Cancer and Non-Tumorigenic

Tissues Reveals Cancer-, Stage- and EGFR-Specific Protein N-Glycosylation. *Glycobiology* **2015**, *25*, 1064–1078; DOI:10.1093/glycob/cwv042.

35. Park, J.-J.; Lee, M. Increasing the α 2, 6 Sialylation of Glycoproteins May Contribute to Metastatic Spread and Therapeutic Resistance in Colorectal Cancer. *Gut Liver* **2013**, *7*, 629–641; DOI:10.5009/gnl.2013.7.6.629.
36. de Freitas Junior, J. C. M.; Morgado-Díaz, J. A. The Role of N-Glycans in Colorectal Cancer Progression: Potential Biomarkers and Therapeutic Applications. *Oncotarget* **2015**, *7*, 19395–19413; DOI:10.18632/oncotarget.6283.
37. Birgisson, H.; Edlund, K.; Wallin, U.; Påhlman, L.; Kultima, H. G.; Mayrhofer, M.; Micke, P.; Isaksson, A.; Botling, J.; Glimelius, B.; Sundström, M. Microsatellite Instability and Mutations in BRAF and KRAS Are Significant Predictors of Disseminated Disease in Colon Cancer. *BMC Cancer* **2015**, *15*, 125; DOI:10.1186/s12885-015-1144-x
38. Tran, B.; Kopetz, S.; Tie, J.; Gibbs, P.; Jiang, Z.-Q.; Lieu, C. H.; Agarwal, A.; Maru, D. M.; Sieber, O.; Desai, J. Impact of BRAF Mutation and Microsatellite Instability on the Pattern of Metastatic Spread and Prognosis in Metastatic Colorectal Cancer. *Cancer* **2011**, *117*, 4623–4632; DOI:10.1002/cncr.26086.
39. Tan, E.; Whiting, J.; Xie, H.; Imanirad, I.; Carballido, E.; Felder, S.; Frakes, J.; Mo, Q.; Walko, C.; Permuth, J. B.; Sommerer, K.; Kim, R.; Anaya, D. A.; Fleming, J. B.; Sahin, I. H. *BRAF* Mutations Are Associated with Poor Survival Outcomes in Advanced-Stage Mismatch Repair-Deficient/Microsatellite High Colorectal Cancer. *The Oncologist* **2022**, *27*, 191–197; DOI:10.1093/oncolo/oyab055.
40. Dennis, J.W.; Laferté, S.; Waghorne, C.; Breitman, M.L.; Kerbel, R.S. Beta 1-6 branching of Asn-linked oligosaccharides is directly associated with metastasis. *Science* **1987**, 236:582-5; DOI: 10.1126/science.2953071.
41. Murata, K.; Miyoshi, E.; Kameyama, M.; Ishikawa, O.; Kabuto, T.; Sasaki, Y.; Hiratsuka, M.; Ohigashi, H.; Ishiguro, S.; Ito, S.; Honda, H.; Takemura, F.; Taniguchi, N.; Imaoka, S. Expression of N-Acetylglucosaminyltransferase V in Colorectal Cancer Correlates with Metastasis and Poor Prognosis. *Clinical Cancer Research* **2000**, *6*, 1772–1777.
42. Kim, Y.-S.; Hwang, S. Y.; Kang, H.-Y.; Sohn, H.; Oh, S.; Kim, J.-Y.; Yoo, J. S.; Kim, Y. H.; Kim, C.-H.; Jeon, J.-H.; Lee, J. M.; Kang, H. A.; Miyoshi, E.; Taniguchi, N.; Yoo, H.-S.; Ko, J.-H. Functional Proteomics Study Reveals That N-Acetylglucosaminyltransferase V Reinforces the Invasive/Metastatic Potential of Colon Cancer through Aberrant Glycosylation on Tissue Inhibitor of Metalloproteinase-1*. *Molecular & Cellular Proteomics* **2008**, *7*, 1–14; DOI:10.1074/mcp.M700084-MCP200.
43. Carvalho, S.; Reis, C. A.; Pinho, S. S. Cadherins Glycans in Cancer: Sweet Players in a Bitter Process. *Trends in Cancer* **2016**, *2*, 519-531; DOI:10.1016/j.trecan.2016.08.003.
44. Brockhausen, I.; Kuhns W. Role and Metabolism of Glycoconjugate Sulfation. *Trends in Glycoscience and Glycotechnology*, 1997, 9, 379–98; DOI: 10.4052/tigg.9.379.
45. Chandrasekaran, E. V.; Xue, J.; Piskorz, C.; Locke, R. D.; Tóth, K.; Slocum, H. K.; Matta, K. L. Potential Tumor Markers for Human Gastric Cancer: An Elevation of Glycan:Sulfotransferases and a Concomitant Loss of A1,2-Fucosyltransferase Activities. J *Cancer Res Clin Oncol* **2007**, 133, 599–611; DOI: 10.1007/s00432-007-0206-0.
46. Capon, C.; Wieruszeski, J.-M.; Lemoine, J.; Byrd, J. C.; Leffler, H.; Kim, Y. S. Sulfated Lewis X Determinants as a Major Structural Motif in Glycans from LS174T-HM7 Human Colon Carcinoma Mucin. *Journal of Biological Chemistry* **1997**, *272*, 31957–31968; DOI:10.1074/jbc.272.51.31957.
47. Horlacher, T.; Oberli, M. A.; Werz, D. B.; Kröck, L.; Bufali, S.; Mishra, R.; Sobek, J.; Simons, K.; Hirashima, M.; Niki, T.; Seeberger, P. H. Determination of Carbohydrate-Binding Preferences of Human Galectins with Carbohydrate Microarrays. *ChemBioChem* **2010**, *11*, 1563–1573; DOI:10.1002/cbic.201000020.
48. Hittelet, A.; Legendre, H.; Nagy, N.; Bronckart, Y.; Pector, J.-C.; Salmon, I.; Yeaton, P.; Gabius, H.-J.; Kiss, R.; Camby, I. Upregulation of Galectins-1 and -3 in Human Colon Cancer and Their Role in Regulating Cell Migration. *International Journal of Cancer* **2003**, *103*, 370–379; DOI:10.1002/ijc.10843.
49. Peng, K.-Y.; Jiang, S.-S.; Lee, Y.-W.; Tsai, F.-Y.; Chang, C.-C.; Chen, L.-T.; Yen, B. L. Stromal Galectin-1 Promotes Colorectal Cancer Cancer-Initiating Cell Features and Disease Dissemination Through SOX9 and β-Catenin: Development of Niche-Based Biomarkers. *Frontiers in Oncology* **2021**, *11*; DOI:10.3389/fonc.2021.716055.
50. Holst, S.; Deuss, A. J. M.; van Pelt, G. W.; van Vliet, S. J.; Garcia-Vallejo, J. J.; Koeleman, C. A. M.; Deelder, A. M.; Mesker, W. E.; Tollenaar, R. A.; Rombouts, Y.; Wuhrer, M. N-Glycosylation Profiling of Colorectal Cancer Cell Lines Reveals Association of Fucosylation with Differentiation and Caudal Type Homebox 1 (CDX1)/Villin MRNA Expression. *Mol Cell Proteomics* **2016**, *15*, 124–140; DOI:10.1074/mcp.M115.051235.
51. Holst, S.; Wilding, J. L.; Koprowska, K.; Rombouts, Y.; Wuhrer, M. N-Glycomic and Transcriptomic Changes Associated with CDX1 MRNA Expression in Colorectal Cancer Cell Lines. *Cells* **2019**, *8*, 273; DOI:10.3390/cells8030273.

52. Guo, R.J.; Suh, E.R.; Lynch, J.P. The role of Cdx proteins in intestinal development and cancer. *Cancer Biol Ther* **2004**, 3, 593-601; DOI: 10.4161/cbt.3.7.913
53. Sethi, M. K.; Thaysen-Andersen, M.; Smith, J. T.; Baker, M. S.; Packer, N. H.; Hancock, W. S.; Fanayan, S. Comparative *N* -Glycan Profiling of Colorectal Cancer Cell Lines Reveals Unique Bisecting GlcNAc and α-2,3-Linked Sialic Acid Determinants Are Associated with Membrane Proteins of the More Metastatic/Aggressive Cell Lines. *J. Proteome Res.* **2014**, *13*, 277–288; DOI:10.1021/pr400861m.
54. Raffaghello, L.; Dazzi, F. Classification and Biology of Tumour Associated Stromal Cells. *Immunology Letters* **2015**, *168*, 175–182; DOI:10.1016/j.imlet.2015.06.016.